Available online at www.sciencedirect.com
SCIENCE DIRECT
Journal of Non-Crystalline Solids 352 (2006) 2399–2403
JOURNAL OF NON-CRYSTALLINE SOLIDS
www.elsevier.com/locate/jnoncrysol

Materials for high-power fiber lasers

J. Kirchhof *, S. Unger, A. Schwuchow, S. Grimm, V. Reichel

Institut für Physikalische Hochtechnologie e.V., Optics Division, Albrecht-Einstein-Strasse 9, PF 100 239, 07702 Jena, Germany

Available online 24 May 2006

Abstract

The absorption and emission properties of silica based ytterbium doped preforms, made by Modified Chemical Vapor Deposition, and of the drawn fibers were investigated as a function of the atmosphere during the preform collapsing. Under increasingly reducing conditions for the collapsing atmosphere, a strong UV/VIS absorption is built up, accompanied with an UV excited emission in the visible region, obviously induced by the formation of Yb^{2+} ions. Both the fluorescence lifetime of the Yb^{3+} lasing level and the cooperative fluorescence in the visible are remarkably diminished. Laser power experiments with the different fibers show a strong deterioration of the laser efficiency parallel to the degree of reduction of the doped glasses.

PACS: 42.55.Wd; 42.81.Bm; 78.55.Hx; 81.40.Tv

Keywords: Oxidation; Reduction; Optical fibers; Lasers; Optical spectroscopy; Silica; Rare-earths in glasses

1. Introduction

Recently, the performance of rare earth doped high-power silica fiber lasers has been dramatically increased with output powers beyond 1 kW, high efficiency and excellent beam quality [1,2]. This progress is due to new design concepts as non-symmetrical double clads and large mode area core structures [3,4]. Relatively little attention, however, has been paid up to now to the influence of material composition, impurities and atomic defects [5], although the extreme power load and complicated fiber structures make high demands on material and preparation technology.

Yb^{3+} is the favorite lasing ion because of the long lifetime of the excited state, the simple energy-level scheme and the small quantum defect between the pump and laser wavelength. Silica glass and high silica glasses, made by gas phase deposition processes, have the main importance as host glass so far because of their unequalled properties such as extremely low optical losses, high radiation hardness and extraordinary mechanical strength, although silica is in principle not very advantageous as host for rare-earths and as laser medium, and its properties must be improved by suitable co-doping [5]. High-power laser fibers are mostly prepared by modified chemical vapor deposition (MCVD) and solution doping within a carrier tube, see e.g. [6], but other preparation routes as outside vapor deposition [7], direct nanoparticle deposition [8] and sintering/melting techniques [9] are also under development.

The present work will contribute to the knowledge of influences of material and preparation technology on the efficiency of high-power laser fibers. Several samples were prepared with nominally identical compositions and according to the same preparation process, but under variable atmosphere conditions during the last core glass preparation step at high temperatures. The absorption and emission properties of the bulk samples (preforms) and the drawn optical fibers where investigated and characterized concerning the resulting lasing properties.

2. Experimental

2.1. Preparation of the specimen

The fiber preform samples have been prepared by MCVD and solution doping according to the following

* Corresponding author. Tel.: +49 36 4120 6204; fax: +49 36 4120 6299.
E-mail address: johannes.kirchhof@ipht-jena.de (J. Kirchhof).

0022-3093/$ - see front matter © 2006 Elsevier B.V. All rights reserved.
doi:10.1016/j.jnoncrysol.2006.02.061

route. At first, a flocculent deposit was formed from a gaseous mixture of $SiCl_4$, $POCl_3$ and O_2 on the inner surface of quartz glass carrier tubes with outer and inner diameter of 14 and 11.5 mm, respectively. This deposit was presintered in a pure oxygen atmosphere at a temperature of 1330 °C in order to generate a defined relative density of 20% compared with a fully densified layer. This layer was impregnated with an aqueous solution of $YbCl_3$ and $AlCl_3$, dried in subsequent preparation steps at room temperature and at about 1000 °C, again in a pure oxygen atmosphere, and at 1400 °C under Cl_2/O_2 atmosphere. After a sintering step at 2000 °C with O_2, a glassy layer with a thickness of about 12 μm was built up on the inner tube surface.

In order to complete the fiber preform, the tube was collapsed by two burner passes at about 2250 °C to a solid rod where the doped layers have formed the preform core with a diameter of about 0.7 mm (outer preform diameter 8 mm). In the standard case, the collapsing has been accomplished in a Cl_2/O_2 atmosphere. (As usual in the MCVD process, all steps have been performed with a moving oxy-hydrogen torch and a flowing gas atmosphere inside the tube-disregarding the last collapsing step.) By changing the gas atmosphere, as described in Table 1, the properties of the core glass were modified.

The preform samples were characterized by nondestructive measurement of the refractive index profile, and by X-ray microscopic analysis on thin preform slices. The ytterbium content was 0.4 mol% Yb_2O_3, codoped with 0.5 mol% P_2O_5 and 4 mol% Al_2O_3. Preform samples have also been used for fluorescence investigations.

From the preforms, fibers have been directly drawn with a velocity of 10 m/min at a drawing tension of about 20p, and characterized by attenuation measurements and spectrally and temporally resolved fluorescence investigation. The fiber core and cladding diameters were about 10 and 125 μm.

For cladding-pumped laser experiments, some preforms have been jacketed with a second quartz glass tube in order to increase the cladding-core relation. Fibers from these preforms had a core diameter of 10 μm and an outer diameter of 400 μm. These fibers were coated with a silicon rubber which had a refractive index lower than silica, leading to a pump clad with a NA of 0.35.

The modifications of the preparation process are shown in Table 1, together with the measured fiber background attenuations in the NIR.

Table 1
Preform/fiber samples

	Doping	Collapsing atmosphere	Fiber loss α (1200 nm)/cm^{-1}	Visual appearance
a	Yb/Al/P	90% O_2/10% Cl_2	0.00003	Homogeneous, colorless
b	Yb/Al/P	He	0.00009	Homogeneous, light yellow
c	Yb/Al/P	90% He/10% CO	0.00012	Homogeneous, light yellow
d	Yb/Al/P	70% Ar/30% CO	0.00017	Homogeneous, dark yellow
e	Yb/Al/P	CO	0.01000	Inhomogeneous, dark yellow
f	Yb/Al/P	95% Ar/5% H_2	0.00032	Homogeneous, dark yellow
g	Yb/Al/P/Ge	He	0.00005	Homogeneous, light yellow
h	–/Al/P	90% O_2/10% Cl_2	0.00001	Homogeneous, colorless
k	–/Al/P	He	0.00001	Homogeneous, colorless
l	–/Al/P	90% He/10% CO	0.00002	Homogeneous, colorless

2.2. Optical characterization

For the absorption measurements on preforms, small polished slices with a thickness d between 1 and 2 mm (in dependence on the expected absorption effect) were illuminated by the collimated beam of a combined halogen/deuterium lamp. Immediately at the back of the sample, the transmitted light was introduced into a fiber probe with core diameter of 600 μm (transmission window from 200 to 1200 nm) and guided to the spectrometer. The exponential absorption coefficients α were determined by comparison of the signal intensity behind the preform core, I, and the pure silica preform cladding, I_0, as $\alpha = \ln(I_0/I)/d$.

For the attenuation measurements on fibers, the focused beam of the lamp was launched into the fiber core and directly guided to the spectrometer. Absorption coefficients were determined by the cut-back method, comparing the output signal intensity of a long and a short fiber length. The exponential absorption coefficients can be converted into the common fiber loss unit dB/km or dB/m according to $\alpha^*[\mathrm{dB\,m^{-1}}] = 434 \cdot \alpha\,[\mathrm{cm^{-1}}]$.

For the measurement of the spectral fluorescence, the 1 mm thick preform slices were arranged in parallel with the collimated beam of a deuterium lamp ('UV excited fluorescence') or the slightly focused monochromatic beam of a cw diode laser system MOPA SDL 8630 ('NIR excited fluorescence', pump wavelength $\lambda_p = 976$ nm). In both cases, emitted light from the preform core was collected and guided to the spectrometer by the above mentioned probe fiber, adjusted perpendicularly to the optical axis of the exciting beam. For the Yb^{3+} emission around 1 μm, fluorescence lifetimes have been determined by time-resolved fluorescence measurements both on preform and fiber samples in a similar kind as described above, using a pulsed MOPA source at 976 nm wavelength with a pulse width of 24 ms at 10 Hz and an InGaAs detector with oscilloscope. Because at the preform sample with thickness of 1 mm already remarkable re-absorption effects disturb the temporal behaviour, here only the results on fibers (with small cores) are presented. All measurements have been done at room temperature.

2.3. Laser experiments

The fibers with core diameter of 10 μm and cladding diameter of 400 μm have been used to construct fiber lasers, using a dielectric mirror at the entrance and the fiber end face as laser mirror at the fiber output. The fiber was cladding-pumped with a fiber coupled diode laser pump system at 976 nm wavelength.

3. Results

3.1. Preform and fiber absorption

All Yb doped preform samples show the typical Yb^{3+} absorption in the wavelength region between 800 and 1100 nm with a broad peak at about 920 nm and a small higher peak at 975 nm, an example is given in the insert of Fig. 1. It is well known that both the spectral shape and the absolute absorption cross sections of Yb^{3+} show a certain distinct dependence on the kind and concentration of co-doping elements [5]. Here however, the different modifications of the preparation process result in no remarkable change of the absorption coefficient, which is about 4 cm^{-1} in the maximum at 975 nm.

In contrast to the NIR absorption, important changes are observed in the UV/VIS region (Fig. 1). The Yb related UV edge shifts partially to longer wavelength and an additional band system builds up with increasingly reducing conditions during the preform collapse, with maxima which are located at about 300 nm, more distinctly at 326 nm, and virtually at about 400 nm. The tail of these absorptions extends in the visible region and is responsible for the increasing yellow colour of the preform cores. Not shown here, that the tail extends till the NIR region (beyond the Yb^{3+} absorption), which leads to a remarkable increase of the fiber background loss. The values of the fiber absorption coefficients, at 1200 nm wavelength, are given in the Table 1. Obviously, the background absorption is still more than two orders of magnitude lower than the Yb^{3+} absorption, but the fiber attenuation increases from about 10 dB/km (standard sample) to values higher than 5000 dB/km for strongly reduced samples. Apart from the sample treated with 100% CO, there is a very good correlation between the absorption coefficients in the UV/VIS and the excess absorption (in comparison to the standard sample) in the NIR at 1200 nm, which confirms that the background absorption is really caused by the tail of the UV/VIS absorption bands. For the peaks at 326–400 nm, respectively, and the absorption at 1200 nm, it holds

$$\lg(\alpha[326]) = \lg(\alpha_{exc}[1200]) + 5.31 \pm 0.07, \quad (1)$$

$$\lg(\alpha[400]) = \lg(\alpha_{exc}[1200]) + 4.74 \pm 0.07. \quad (2)$$

The sample which was strongly treated with CO shows inhomogeneous structure by coarse composition fluctuations which gives rise to additional scattering losses. This sample is not considered in the following.

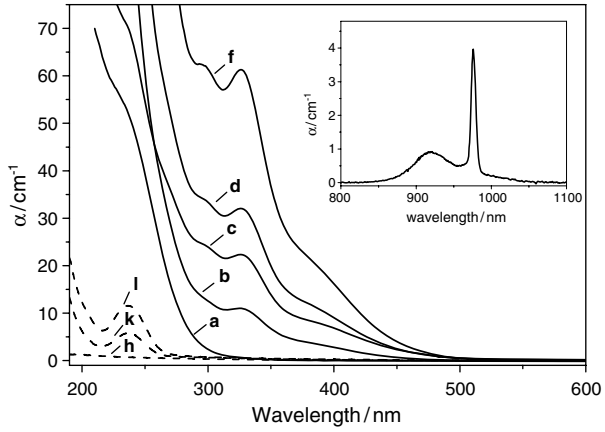

Fig. 1. Preform absorption spectra in UV/VIS and NIR (inset).

3.2. Yb^{3+} near infrared fluorescence

With excitation at 976 nm, all investigated samples show the typical emission spectrum between 900 and 1150 nm for the transition between the $^2F_{5/2}$ multiplet manifold and the $^2F_{7/2}$ ground state [5]. The shape of the spectrum is hardly affected by the modifications during the preparation. In contrast to the invariable spectral behaviour, the fluorescence lifetime is decreased in consequence of the reducing treatment, and the decay kinetics, which is purely exponential in the case of the standard sample, must be described by two or more components, see Table 2.

3.3. NIR excited visible fiber fluorescence

A typical feature of Yb doped materials is the visible emission peaked near 500 nm wavelength, if the Yb^{3+} is excited in the absorption maximum at 976 nm. This emission is responsible for the intensive green shining of a lasing fiber. It is explained as cooperative luminescence, where a pair of excited Yb^{3+} ions emits one photon with the double energy of the absorption transition [10,11].

As shown in Fig. 2, the reducing conditions lead to a strong decrease of the cooperative luminescence.

Table 2
Yb^{3+} near infrared fluorescence lifetimes ($^2F_{5/2} \rightarrow {}^2F_{7/2}$, excitation 976 nm)

	τ (100–37%)/μs	τ (A1)/μs	τ (A2)/μs
a	850	850 (100%)	–
b	800	800 (100%)	–
c	760	801 (92%)	384 (8%)
d	770	812 (92%)	403 (8%)
e	600	680 (83%)	300 (17%)
f	620	684 (86%)	298 (14%)
g	830	878 (79%)	665 (21%)

3.4. UV excited fiber fluorescence

The standard sample, excited with deuterium lamp, shows no measurable emission in the UV and visible region between 200 and 800 nm wavelength. As shown in Fig. 3, the reducing treatment leads in all cases to an emission. The samples without Yb show a peak at 400 nm, obviously in consequence of the oxygen-deficiency absorption at 240 nm (Fig. 1), which is extremely strong in the Ge co-doped material (not shown in Figs. 1 and 3). In the Yb doped samples, this peak seems also to exist, but a stronger emission around 520 nm is successively built up.

3.5. Laser experiments

With three fiber samples, laser experiments have been carried out. As shown in Fig. 4, the reducing treatment leads to a surprisingly strong decrease of the laser efficiency.

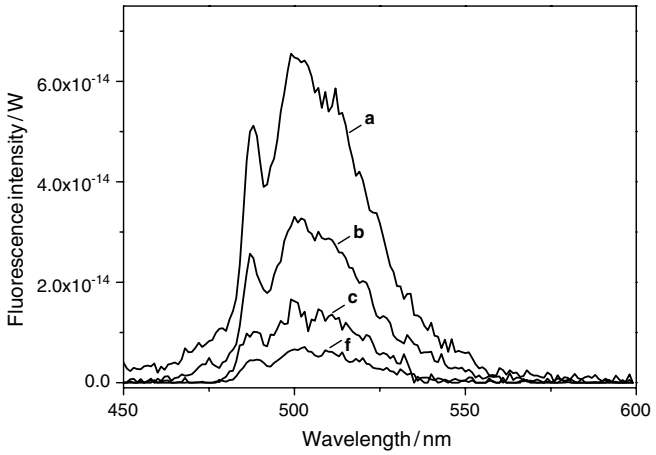

Fig. 2. NIR excited visible emission spectra (excitation 976 nm).

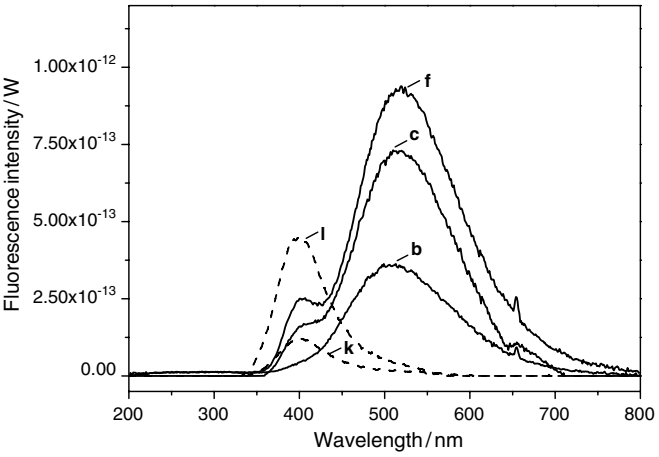

Fig. 3. UV excited visible emission spectra (excitation deuterium lamp).

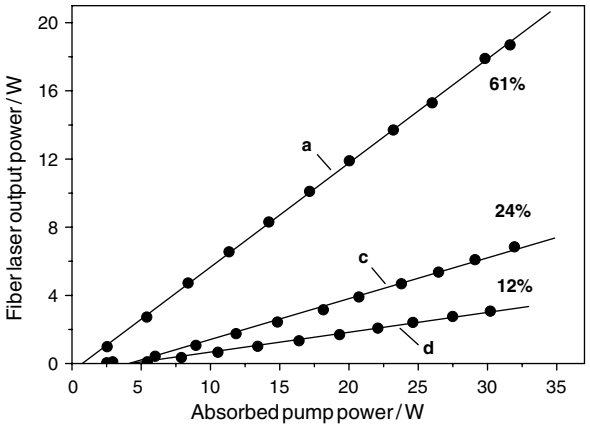

Fig. 4. Fiber laser characteristic curves (pump wavelength 976 nm).

4. Discussion

It is well known, that the atmosphere during collapsing of MCVD layers can influence the properties of the preform and fiber core material despite of the fact that a fully vitrified layer has been formed already before the collapse step [12]. This is owing to the small layer thickness of about 10 μm in combination with the high processing temperatures of about 2200 °C which enhance in- and out-diffusion of volatile species and solid state reactions. It can be estimated from the spatial and temporal conditions of collapsing, that species with a diffusion coefficient of $\geqslant 10^{-8}$ cm^2 s^{-1} can significantly diffuse in the core layers. This is true for molecular hydrogen [13], but also for molecular oxygen [14] and probably for CO and other molecules with similar size.

The different atmospheres used here give rise to an oxygen deficient glass state, increasing in the order He–CO–H_2, as shown from the absorption spectra (Fig. 1) and the emission spectra with UV excitation (Fig. 3) [15]. Much more important, however, are the Yb related phenomena, characterized by an absorption band system between 300 and 400 nm, accompanied with the UV excited emission at about 500 nm. Probably, these effects are connected with the increasing formation of Yb^{2+} ions in the chemically reduced glass matrix, compare e.g. [16,17]. The consequence of this reduced state is on the one hand an increased background loss of the laser fiber, which is remarkably but nevertheless assumed to be without important influence on the lasing effect because the Yb^{3+} gain is high and the used fibers are only some tens of meters long. On the other hand, however, the increasingly reduced state influences directly the lasing level, as seen from the fluorescence lifetimes (Table 2) and the vanishing cooperative luminescence (Fig. 2). In the result, the laser efficiency is drastically impaired (Fig. 4).

The effect of germanium doping is still not investigated in detail (sample *g*). First results indicate that the Ge doping can mitigate to a certain extent the deterioration of the laser properties in the reduced samples. Worthy to note

that a reducing treatment in the same manner as practiced here, in the case of neodymium doping (which is also of interest for high-power fiber lasers) leads to diminished background losses in strong contrast to the behavior of ytterbium [5].

5. Conclusion

A reducing treatment of ytterbium doped silica based glasses impairs their laser properties. This phenomenon can be avoided in the MCVD preparation. It must be carefully considered, however, if other routes are used for the fabrication of high-power laser fibers.

References

[1] Y. Jeong, J.K. Sahu, D.N. Payne, J. Nilsson, Opt. Express 12 (2004) 6088.
[2] K. Mörl, S. Unger, V. Reichel, J. Kirchhof, H. Bartelt, H.-R. Müller, T. Sandrock, A. Harschak, A. Liem, Europhoton-Conference of 'Solid-State and Fiber Coherent Light Sources', Lausanne, Switzerland, 2004.
[3] A. Tünnermann, H. Zellmer, W. Schöne, A. Giesen, K. Contag, New Concepts for Diode-Pumped Solid-State Lasers, in: R. Diehl (Ed.), High-Power Diode Lasers, Springer-Verlag, Berlin Heidelberg, 2000.
[4] A. Tünnermann, S. Höfer, A. Liem, J. Limpert, M. Reich, F. Röser, T. Schreiber, H. Zellmer, Proc. SPIE 5709 (2005) 301.
[5] J. Kirchhof, S. Unger, A. Schwuchow, S. Jetschke, B. Knappe, Proc. SPIE 5723 (2005) 261.
[6] P.C. Becker, N.A. Olsson, J.R. Simpson, Erbium-Doped Fiber Amplifier, Fundamentals and Technology, Academic Press, 1999.
[7] J. Wang, D.T. Walton, L.A. Zenteno, Electron. Lett. 40 (2004) 590.
[8] S. Tammela, P. Kiiveri, S. Särkhilahti, M. Hotoleanu, H. Valkonen, M. Rajala, J. Kurki, K. Janka, Proc. European Conf. on Opt. Comm. 4 (2002) 9.4.2.
[9] J. Kirchhof, S. Unger, J. Kobelke, K. Schuster, K. Mörl, S. Jetschke, A. Schwuchow, Proc. SPIE 5951 (2005) 595107.
[10] E. Nakazawa, S. Shionoya, Phys. Rev. Lett. 25 (1970) 1710.
[11] Y.G. Choi, Y.B. Shin, H.S. Seo, K.H. Kim, Chem. Phys. Lett. 364 (2002) 200.
[12] S. Unger, J. Kirchhof, S. Schröter, A. Schwuchow, H. Frost, Proc. SPIE 4616 (2002) 161.
[13] F.J. Norton, Nature 191 (1961) 701.
[14] J.E. Shelby, J. Appl. Phys. 48 (1977) 3387.
[15] A. Trukhin, B. Poumellec, J. Garapon, J. Non-Cryst. Solids 332 (2003) 153.
[16] S. Lizzo, E.P. Klein Nagelvoort, R. Erens, A. Meijerink, G. Blasse, J. Phys. Chem. Solids 58 (1997) 963.
[17] S. Lizzo, A. Meijerink, G.J. Dirksen, G. Blasse, J. Phys. Chem. Solids 56 (1995) 959.